

Non-equilibration, synchronization, and time crystals in isotropic Heisenberg models

Peter Reimann, Patrick Vorndamme, and Jürgen Schnack
Faculty of Physics, Bielefeld University, 33615 Bielefeld, Germany
(Dated: October 10, 2023)

Isotropic but otherwise largely arbitrary Heisenberg models in the presence of a homogeneous magnetic field are considered, including various integrable, non-integrable, as well as disordered examples, and not necessarily restricted to one dimension or short-range interactions. Taking for granted that the non-equilibrium initial condition and the spectrum of the field-free model satisfy some very weak requirements, expectation values of generic observables are analytically shown to exhibit permanent long-time oscillations, thus ruling out equilibration. If the model (but not necessarily the initial condition) is translationally invariant, the long-time oscillations are moreover shown to exhibit synchronization in the long run, meaning that they are invariant under arbitrary translations of the observable. Analogous long-time oscillations are also recovered for temporal correlation functions when the system is already at thermal equilibrium from the outset, thus realizing a so-called time crystal.

I. INTRODUCTION

A macroscopic system without external perturbations approaches a steady equilibrium state after sufficiently long times, no matter how far from equilibrium it started out. On the phenomenological level, this is an extremely well-established fact both in everyday life and under controlled laboratory conditions. More precisely speaking, in every single run of an experiment, one may still encounter certain statistical or quantum mechanical fluctuations, especially for microscopic observables, but on the average over many repetitions of the experiment, the expectation value will closely approach some constant equilibrium value in the long run. On the other hand, a satisfactory theoretical understanding of these empirical observations in terms of the underlying fundamental laws of quantum mechanics still remains a challenging open question, both qualitatively and quantitatively, to which a considerable amount of experimental, numerical, and analytical efforts have been devoted in recent years [1–6].

Obviously, a particularly fascinating endeavor in this context is to identify cases which give rise to certain deviations from the above-mentioned standard scenario. For instance, it has been discovered that models exhibiting integrability or many-body localization may not entail thermalization, meaning that expectation values do not closely approach the pertinent canonical or microcanonical values predicted by equilibrium statistical mechanics after sufficiently long times [1–6]. Nevertheless, generically they still exhibit equilibration, meaning that the time-dependent expectation values stay extremely close to a constant value for the vast majority of all sufficiently late times, i.e., apart from the transient relaxation processes during some initial time-interval, and apart from the well-known, exceedingly rare but unavoidable quantum recurrence or revival effects [7–13].

At the focus of our present work are many-body systems whose expectation values do not even equilibrate in the above sense, but rather exhibit permanent long-time oscillations. Leaving aside trivial cases like non-

interacting systems or perfect harmonic oscillators, related previously proposed examples that may come to one’s mind are the “quantum Newton’s cradle” experiment by Kinoshita, Wenger, and Weiss [14], the exploration of Rydberg-atom quantum simulators by Bernien et al. [15], or the numerical study by Banuls, Cirac, and Hastings [16]. However, it was later discovered that in fact all those examples ultimately still must exhibit equilibration when monitoring the dynamical evolution over sufficiently long times [17–21]. On the other hand, analytically provable absence of equilibration in the context of many-body quantum scars has been recently established for various abstract models in combination with special initial conditions [18], yet their significance with regard to real-world systems still remains to be explored.

In our present work, we focus on one of the simplest and best-established many-body quantum systems, namely the isotropic Heisenberg model with a homogeneous magnetic field. Besides the original and most common version of the model, also various generalizations and modifications will be covered, including non-integrable systems and disorder in the form of randomized interactions. The only indispensable prerequisites are that the field-free model must be $SU(2)$ symmetric, i.e. isotropic, the external field must be spatially homogeneous, and the energy levels must satisfy some rather weak and generic assumptions.

Our first main objective is to analytically demonstrate and numerically illustrate the typical occurrence of non-equilibration in the form of everlasting oscillations in such systems. In particular, this behavior is restricted neither to special initial conditions nor to integrable models.

Furthermore, we analytically show that those oscillations entail synchronization under the additional condition that the model – but not necessarily the initial condition – is translationally invariant.

Turning to systems at thermal equilibrium, we finally establish the generic occurrence of analogous long-time oscillations for dynamic (time-dependent) correlation functions, and we discuss their implications with respect to the topic of time crystals [22–28].

In terms of these main findings, but also methodologically, our present paper is closely related in a variety of different respects to a considerable number of previous works, including Refs. [7–12, 25–30]. Since an adequate comparison is only possible on the basis of a minimal amount of formal definitions, such a more detailed discussion of pertinent previous works will be provided at various places throughout the paper.

II. GENERAL FRAMEWORK

We consider a Heisenberg model on an arbitrary (not necessarily one-dimensional) lattice, whose sites are labeled by i . We denote by Λ the set of all possible lattice sites, and by κ their total number. Alternatively, κ may thus be viewed as the system size or as the number of degrees of freedom. The single-site spin operators are indicated by vectors \vec{s}_i with three components s_i^a , $a \in \{x, y, z\}$, while the single-site spin quantum number is given by the same integer or half-integer s on every site.

Denoting the components of the total spin by

$$S^a := \sum_{i \in \Lambda} s_i^a, \quad (1)$$

the considered Hamiltonians must be of the general form

$$H := H_0 + h S^z, \quad (2)$$

$$H_0 := \sum_{i,j \in \Lambda} J_{ij} \vec{s}_i \cdot \vec{s}_j, \quad (3)$$

where the magnetic field h and the coupling constants J_{ij} are, for the time being, still largely arbitrary model parameters.

Since the Hamiltonian H_0 in (3) is spatially isotropic, it possesses SU(2) symmetry and thus commutes with S^a for all $a \in \{x, y, z\}$. As a consequence, the eigenvectors of H_0 can be chosen so that they are simultaneously eigenvectors of S^z as well as of $\vec{S}^2 := (S^x)^2 + (S^y)^2 + (S^z)^2$, and thus can be written as $|n, l\rangle$ with the properties

$$H_0 |n, l\rangle = E_n^0 |n, l\rangle, \quad (4)$$

$$S^z |n, l\rangle = l |n, l\rangle, \quad (5)$$

$$\vec{S}^2 |n, l\rangle = L_n(L_n + 1) |n, l\rangle. \quad (6)$$

Here, the indices $n \in \{1, \dots, N\}$ label the energy eigenvalues, the $l \in \{-L_n, \dots, L_n\}$ are the total magnetic quantum numbers, while the L_n are positive integers or half-integers, often denoted as total spin quantum numbers. In other words, for any given n , the energies E_n^0 are $(2L_n+1)$ -fold degenerate with spin multiplets $\{|n, l\rangle\}_{l=-L_n}^{L_n}$. Traditionally, those simultaneous eigenvectors of H_0 , \vec{S}^2 , and S^z are often denoted as $|n, L_n, l\rangle$, but since the L_n 's are unique functions of the n 's, we employ the shorter notation $|n, l\rangle$. One readily verifies that

$0 \leq L_n \leq \kappa s$, and one can evaluate how many eigenvectors belong to a certain l or L_n [31], but for the rest, the actual quantitative value of L_n belonging to any given n (or E_n^0) is in general quite difficult to tell; see also Appendix A. We finally remark that the energies E_n^0 are generically expected to be pairwise different, but that this property is not actually required in most of our subsequent explorations.

Exploiting (2), (4), (5) it follows that

$$H |n, l\rangle = E_n |n, l\rangle, \quad (7)$$

$$E_n l := E_n^0 + l h. \quad (8)$$

The eigenvectors $|n, l\rangle$ are thus independent of h , while the above-mentioned degeneracies of the eigenvalues for $h = 0$ are expected to be generically lifted for $h \neq 0$ (Zeeman splitting).

Given any pure or mixed initial state $\rho(0)$, its time evolution is governed by the von Neumann equation, resulting at time t in the state $\rho(t) = e^{-iHt} \rho(0) e^{iHt}$ ($\hbar = 1$). Accordingly, the expectation value of any observable (Hermitian operator) A at time t is given by

$$\langle A \rangle_t := \text{Tr}\{\rho(t)A\}. \quad (9)$$

By employing the eigenvalues and eigenvectors of H from (7) and (8) it follows that

$$\langle A \rangle_t = \sum_{mnkl} \rho_{mn}^{k,l} A_{nm}^{l,k} e^{i(E_n^0 - E_m^0 + [l-k]h)t}, \quad (10)$$

where the sum is tacitly restricted to indices m, n, k, l within their admitted range as specified below (6), and where the matrix elements $\rho_{mn}^{k,l}$ and $A_{nm}^{l,k}$ are defined as

$$\rho_{mn}^{k,l} := \langle m, k | \rho(0) | n, l \rangle, \quad (11)$$

$$A_{nm}^{l,k} := \langle n, l | A | m, k \rangle. \quad (12)$$

Going over from the summation index l in (10) to $\nu := l - k$ then yields

$$\langle A \rangle_t = \sum_{\nu} f_{\nu}(t) e^{i\nu h t}, \quad (13)$$

$$f_{\nu}(t) := \sum_{mn} e^{i(E_n^0 - E_m^0)t} \sum_k \rho_{mn}^{k, k+\nu} A_{nm}^{k+\nu, k}. \quad (14)$$

One readily verifies that $f_{-\nu}(t) = f_{\nu}^*(t)$, hence (13) could also be rewritten as a purely real Fourier series. Since the eigenvectors $|n, l\rangle$ in (4) and thus in (7) are independent of h , the same property is inherited by the matrix elements in (11) and (12), and finally by the functions $f_{\nu}(t)$ in (14). In other words, the only h -dependence in (13) arises via the exponential factors on the right-hand side.

A. Model classification

The general structure in (1)-(3) still covers a wide variety of models in one or more dimensions, whose interactions may be of short- or long-range character, and may

even exhibit various kinds of disorder with concomitant many-body localization effects [6]. Moreover, also our assumption that all lattice sites exhibit the same spin quantum number s can be readily relaxed.

We emphasize that these models (1)-(3) include many examples which are commonly considered as being either integrable or non-integrable, even though the precise meaning of “integrability” is still not entirely clear [3, 4]. Independently of such still unsettled subtleties, for our present purposes it seems reasonable to require that whether a given model in (1)-(3) is considered as (non-)integrable should *not* depend on the value of the external field h . The reason is that since the eigenvectors in (7) are independent of h , and the dependence of the eigenvalues in (8) on h is rather trivial, it would not be satisfying if a transition from integrable to non-integrable would be achievable by simply changing the value of h .

III. MAIN RESULTS

Our first main result consists in the prediction that, for sufficiently large systems, the expectation values in (13) can be approximated very well by

$$\mathcal{A}_t := \sum_{\nu} \bar{f}_{\nu} e^{i\nu ht} \quad (15)$$

for the vast majority of all sufficiently late times t , where \bar{f}_{ν} essentially amounts to the long-time average of $f_{\nu}(t)$ from (14). More precisely speaking,

$$\bar{f}_{\nu} := \sum'_{mnk} \rho_{mn}^{k,k+\nu} A_{nm}^{k+\nu,k}, \quad (16)$$

where the prime symbol indicates that the summation is restricted to indices m and n with the property $E_m^0 = E_n^0$. In the generic case that all energies E_n^0 are pairwise different (see below Eq. (6)), this boils down to

$$\bar{f}_{\nu} = \sum_{nk} \rho_{nn}^{k,k+\nu} A_{nn}^{k+\nu,k}. \quad (17)$$

More generally, the same simplification (17) of (16) also applies to cases where either $\rho_{mn}^{k,l}$ or $A_{nm}^{l,k}$ vanishes whenever $m \neq n$ and $E_m^0 = E_n^0$ (degeneracies). We also recall that similar restrictions as below (10) are understood to apply to the sums in (16) and (17).

Before providing the quantitative analytical details of the above prediction, let us mention a non-rigorous argument of how the emergence of such a result may be intuitively understood:

Indicating the average over all times $t \geq 0$ by $\langle \cdot \rangle_{\infty}$, we can conclude that $\langle e^{i(E_n^0 - E_m^0)t} \rangle_{\infty}$ equals unity if $E_m^0 = E_n^0$ and zero otherwise. Together with (14) and (16) it follows that $\langle f_{\nu}(t) \rangle_{\infty} = \bar{f}_{\nu}$. Moreover, for sufficiently large systems, the number of summands on the right-hand side of (14) may be expected to become very large. Incidentally, in view of the restrictions mentioned below Eq. (10), a

more rigorous justification of this argument for any single ν may be difficult. Taking it for granted nevertheless, the key point now consists in the heuristic conjecture that this large number of summands in (14) entails some kind of “dephasing effect”, with the result that all the summands with $E_m^0 \neq E_n^0$ effectively cancel each other in sufficiently good approximation. As a consequence, every $f_{\nu}(t)$ in (14) is conjectured to stay near its time average (16), and hence the expectation values (13) to stay near \mathcal{A}_t from (15).

Next we turn to a more rigorous foundation of our prediction. In doing so, we proceed in three steps. First, the two most important quantities appearing in our main analytical result are introduced. Next, the analytical result itself is presented and discussed. Finally, the actual derivation of the result is provided in Appendix A.

For an instructive numerical illustration of those general predictions, we refer to Sec. III E.

A. Level populations and energy gaps

According to the first remark below Eq. (8), the quantity $\langle n, l | \rho(0) | n, l \rangle$ is independent of the magnetic field h . Moreover, it can be identified with the population of the energy eigenstate $|n, l\rangle$ by the initial state $\rho(0)$. Likewise,

$$p_{\max} := \max_{n,l} \langle n, l | \rho(0) | n, l \rangle \quad (18)$$

thus amounts to the *maximal level population* and is h -independent. We also note that the corresponding time-dependent level populations $\langle n, l | \rho(t) | n, l \rangle$ are actually independent of t , as can be seen by rewriting them in the form (9) with $A := |n, l\rangle\langle n, l|$ and then exploiting (10).

Next we focus on an arbitrary but fixed pair of indices (m, n) with the property $E_m^0 \neq E_n^0$, and we count all possible index pairs (m', n') whose energy gaps $E_{m'}^0 - E_{n'}^0$ are equal to the given reference gap $E_m^0 - E_n^0$. The number of those pairs (m', n') is denoted as γ_{mn}^0 . For obvious reasons, this number γ_{mn}^0 is called the degeneracy of the energy gap $E_m^0 - E_n^0$, and it has the properties that $\gamma_{mn}^0 \geq 1$ and $\gamma_{nm}^0 = \gamma_{mn}^0$. Specifically, if $\gamma_{mn}^0 = 1$ then $E_m^0 - E_n^0$ is called a non-degenerate energy gap. Finally, the *maximal energy gap degeneracy* is defined as

$$\gamma^0 := \max_{m,n} \gamma_{mn}^0, \quad (19)$$

where the maximum is taken over all pairs (m, n) with non-vanishing energy gaps $E_m^0 - E_n^0$ [11].

We close with two side remarks: (i) The above defined quantities γ_{mn}^0 and γ^0 refer, as indicated by the superscript “0”, to the unperturbed system, and as such are independent of h for trivial reasons. (ii) As already mentioned below (6), we do not require that all E_n^0 are pairwise different, with the following implication with regard to γ^0 : Denoting for any given n the number of indices k with the property $E_k^0 = E_n^0$ by $\mu(n)$ (“multiplicity of E_n^0 ”) it readily follows that $\gamma_{mn}^0 \geq \mu(m)\mu(n)$, and hence

that $\gamma^0 \geq \mu_{\max}^2$, where $\mu_{\max} := \max_n \mu(n)$ is the maximal number of pairwise identical energies E_n^0 . Even for integrable systems such as spin-1/2 rings the maximal number of pairwise identical energies increases only by a factor of order 2 and only in certain Hilbert-subspaces [32]. On the other hand, even if all E_n^0 are pairwise different and thus $\mu_{\max} = 1$, it is still possible that $\gamma^0 > 1$.

B. Main analytical prediction

Employing the definitions (18) and (19), and indicating the temporal average over an interval $[0, T]$ by the symbol $\langle \cdot \rangle_T$, it is shown in Appendix A that the mean square deviation of the “true” expectation values (13) from the auxiliary function (15) obeys for all sufficiently large T the inequality

$$\langle [\langle A \rangle_t - \mathcal{A}_t]^2 \rangle_T \leq \gamma^0 (2s\kappa + 1)^2 \Delta_A^2 p_{\max}, \quad (20)$$

where s is the single-spin quantum number and κ the system size (see above Eq. (1)). Furthermore, Δ_A is the measurement range of the observable A , i.e., the difference between the largest and smallest possible measurement outcomes, or equivalently, eigenvalues of A .

Our first remark is that the right-hand side of (20) is independent of the magnetic field h in (2).

Our second remark is that the level density of a many-body system is commonly known or expected [2, 4, 33] to grow exponentially fast with the system size κ . Hence, the level density will become extremely high for macroscopically large systems, and it will be practically impossible in a real experiment to notably populate only a small number of eigenstates $|n, l\rangle$. Rather, one expects [7, 10, 12] that the number of non-negligibly populated levels will still be exponentially large in κ . Recalling Eq. (18), and that the sum of all level populations must be unity, one thus expects [7, 10, 12] that a very rough order of magnitude estimate of the form

$$p_{\max} \approx \exp\{-\mathcal{O}(\kappa)\} \quad (21)$$

will be generically fulfilled under all experimentally realistic circumstances. For some particularly important examples, a more detailed confirmation of this property will be provided in Sec. III C below.

Our third remark is that, obviously, no significant conclusion about the expectation values in (10) can be drawn without any knowledge whatsoever regarding the energies E_n^0 appearing on the right-hand side. On the other hand, these energies are in general not explicitly known in sufficient quantitative detail. An exception is given by models that are analytically solvable by means of the Bethe ansatz, but in practice this is of little use for our present purposes. For instance, already one of the simplest and most important features of the energies E_n^0 , namely the so-called level statistics (probability distribution of the distances between neighboring energy levels), is not analytically available for practically any quantum many-body system of physical interest, including our

present Heisenberg models of the general form (2). However, it is commonly taken for granted – based on heuristic arguments and ample numerical evidence – that the level statistics tends to some well-defined and reasonably smooth asymptotics in the thermodynamic limit. Moreover, this asymptotics is often expected to be close to, for instance, a Wigner-Dyson or a Poisson distribution, but such “details” do not matter here.

Our present assumption regarding the energies E_n^0 is in essence quite similar in spirit to these common assumptions regarding the level statistics. Namely, we assume that the maximal energy gap degeneracy in (19) grows at most subexponentially with the system size κ . Indeed, this is closely related to requiring that the level statistics does not develop delta-peaks in the thermodynamic limit. In particular, this also means that the maximal number of pairwise identical energies E_n^0 must grow at most subexponentially with κ , see remark (ii) at the end of Sec. III A.

Finally, it is also noteworthy that our above assumptions regarding p_{\max} and γ^0 are by now very well-established in the context of equilibration in many-body quantum systems, and that there exists essentially no rigorous analytical result in this context which is valid without taking for granted the same or some very similar assumptions [2, 3, 7–12, 21, 34–39].

Altogether, we thus can and will take our above assumptions regarding p_{\max} and γ^0 for granted. For large κ , the small factor p_{\max} in (21) then overrules by far the factors γ^0 and κ^2 on the right-hand side of (20), implying that the time-averaged variance on the left-hand side of (20) will be exponentially small compared to the (squared) measurement range Δ_A of the observable. In turn, this is only possible if the difference $\langle A \rangle_t - \mathcal{A}_t$ is unmeasurably small (below the resolution limit of the measurement device A) for the overwhelming majority of all time points $t \in [0, T]$. As already said in the Introduction, time points t belonging to the complementary, exceedingly small minority are generically expected to occur during the initial transient relaxations processes, and on the occasion of the well-known, exceedingly rare, but unavoidable quantum recurrences or revivals, see, e.g., Ref. [13] and further references therein. The initial relaxation may in fact be viewed as one of them. Moreover, the origin of those revivals is closely related to the fact that the sum in (10) is a quasi-periodic function of t . All these complications are effectively taken into account by our requirement above (20) that T must be sufficiently large.

In summary, our main finding is that the deviations between $\langle A \rangle_t$ and \mathcal{A}_t will be negligibly small for the overwhelming majority of all sufficiently late times t , symbolically indicated as

$$\langle A \rangle_t \rightsquigarrow \mathcal{A}_t. \quad (22)$$

Incidentally, similar methods as in the derivation of our present result in Appendix A have been previously adopted, e.g., in Ref. [7–12] in the context of *equilibra-*

tion, i.e., for the purpose to show that the expectation values $\langle A \rangle_t$ remain – under suitable conditions on the Hamiltonian H , the initial state $\rho(0)$, and the observable A – very close to some *constant* value for the vast majority of all sufficiently late times t . Obviously, such a prediction of equilibration cannot apply to our present models (2) with $h \neq 0$ since they generically give rise to everlasting oscillations of $\langle A \rangle_t$, see also Sec. III D below. The main reason is that the energies E_{nl} in (8) violate (for $h \neq 0$) the corresponding requirements in Refs. [7–12] regarding the maximally admissible degeneracy of the pertinent energy gaps. Indeed, one finds that our present models entail some exponentially large sets of degenerate energy gaps: For instance, considering two arbitrary but fixed indices l and l' we can conclude from Eq. (8) that the energy gaps $E_{nl} - E_{n'l'}$ are equal for all possible values of n , while the total number of all those n values is often expected to be exponential in the system size. Likewise, for any given set of indices n, l, n', l' the energy gaps $E_{n(l+l'')} - E_{n'(l'+l'')}$ are equal for all possible values of l'' . As a consequence, for $h \neq 0$ our models violate one of the central preconditions for equilibration established in Refs. [7–12].

In contrast, the maximal degeneracy of energy gaps employed in (19) is a property of the *unperturbed* ($h = 0$) energies E_n^0 , *not* of the energies E_{nl} pertaining to the actually considered model Hamiltonian H in (2) with $h \neq 0$. In passing, we also remark that, according to Refs. [7–12], it is the degeneracy of these gaps for $h \neq 0$ which prohibits equilibration, *not* their commensurability, as speculated, e.g., in [40].

C. Canonical quenches

In view of (18) we can conclude that $(p_{\max})^2$ is upper bound by $\sum_{nl} \langle n, l | \rho(0) | n, l \rangle^2$ and hence by $\sum_{nlmk} |\langle n, l | \rho(0) | m, k \rangle|^2 = \text{Tr}\{[\rho(0)]^2\}$, implying

$$p_{\max} \leq \sqrt{\text{Tr}\{[\rho(0)]^2\}}. \quad (23)$$

As a particularly simple and interesting example, let us assume that the initial state is given by a thermal Gibbs state (canonical ensemble) of the form

$$\rho(0) = \tilde{Z}^{-1} e^{-\beta \tilde{H}}, \quad \tilde{Z} := \text{Tr}\{e^{-\beta \tilde{H}}\}, \quad (24)$$

where \tilde{H} is in general different from the Hamiltonian H in (2) which governs the subsequent temporal evolution of $\rho(0)$.

For instance, one may choose \tilde{H} to be of the general form

$$\tilde{H} := H_0 + \sum_{i \in \Lambda} \vec{h}_i \cdot \vec{s}_i, \quad (25)$$

thus differing from H in (2) with respect to the direction and possibly also the magnitude of the externally applied

magnetic field at any of the lattice sites i . Further examples of how to choose physically reasonable \tilde{H} 's are rather obvious, see also Sec. III E below.

From a different viewpoint, the system may thus be considered as being at thermal equilibrium for $t < 0$ and experiencing an instantaneous “quantum quench” at $t = 0$, with pre-quench Hamiltonian \tilde{H} and post-quench Hamiltonian H .

Exploiting that the free energy F_β associated with the canonical ensemble (24) obeys the relation $e^{-\beta F_\beta} = \text{Tr}\{e^{-\beta \tilde{H}}\}$, one can conclude that $\text{Tr}\{[\rho(0)]^2\} = e^{-2\beta G_\beta}$ with $G_\beta := F_{2\beta} - F_\beta$. Taking for granted that the pre-quench system exhibits generic thermodynamic properties, it follows that G_β is an extensive quantity. Hence, $\text{Tr}\{[\rho(0)]^2\}$ decreases exponentially with the system size κ , and likewise for p_{\max} in (23).

Altogether, we thus have rigorously verified (21) for initial conditions of the canonical form (24). The same conclusion can also be readily recovered for microcanonical instead of canonical initial states $\rho(0)$.

D. Permanent oscillations

To begin with, we note that \bar{f}_ν in (16) must be zero if $|\nu| > 2\kappa s$ as a consequence of the restrictions on the summation indices below (10) (the detailed reasoning is worked out below Eq. (A14)). Furthermore, one can infer from (11), (12), and (16) that $\bar{f}_{-\nu} = \bar{f}_\nu^*$. Representing the complex numbers \bar{f}_ν in the polar form $|\bar{f}_\nu| e^{i\varphi_\nu}$, we thus can rewrite (15) as

$$\mathcal{A}_t = \bar{f}_0 + 2 \sum_{\nu=1}^{2\kappa s} |\bar{f}_\nu| \cos(\nu ht + \varphi_\nu). \quad (26)$$

Generically, the quantities \bar{f}_ν in (16) are not expected to identically vanish for all $\nu \neq 0$, hence (26) together with (22) implies the occurrence of permanent oscillations for all sufficiently late times t . Exceptional cases, tailored such that $\bar{f}_\nu = 0$ for all $\nu \neq 0$, will be addressed later in Sec. VI.

As an aside, we remark that the quantity \bar{f}_0 in (26) obviously represents the long-time average of \mathcal{A}_t . In the generic case that all energies E_n^0 are pairwise different (see also below Eq. (6)), \bar{f}_0 can be further rewritten by means of (17) and the so-called *diagonal ensemble*

$$\rho_{\text{dia}} := \sum_{nl} \rho_{nn}^{l,l} |n, l\rangle \langle n, l| \quad (27)$$

in the form

$$\bar{f}_0 = \text{Tr}\{\rho_{\text{dia}} A\}. \quad (28)$$

We also remark that our present oscillatory long-time effects are similar to those recently discovered in the ground-breaking work [25]. A first important difference is that Ref. [25] is mainly focused on the one-dimensional

spin-1/2 XXZ-model (which is integrable), while our present model class also covers, for instance, various non-integrable and disordered systems (cf. Sec. II A). The second important difference is that the findings reported in Ref. [25] are mainly based on non-rigorous arguments and numerical evidence, adopting some rather special initial states and observables. Finally, the prediction of permanent oscillations in Ref. [25] only applies to a quite restricted (discrete) subset of the XXZ spin chain's anisotropy parameter values.

E. Numerical examples

The subsequent numerical examples are chosen to illustrate our two main analytical findings for Hamiltonians of the general form (1)-(3): (I) permanent oscillations, and (II) synchronization of these oscillations in case of translationally invariant Hamiltonians, see also Sec. IV below. To this end, we numerically explore the behavior of the following four specific models: (i) A spin ring (i.e. periodic boundary conditions) with unperturbed Hamiltonian

$$H_0 := \sum_{i=1}^{\kappa} J_i \vec{s}_i \cdot \vec{s}_{i+1} , \quad (29)$$

exhibiting quenched disorder by choosing the interactions J_i as independent, identically distributed random numbers. (ii) The same spin ring model as in (29), but now with identical couplings J_i for all i (no disorder). (iii) A two-dimensional (2D) 5×5 square lattice model with identical nearest-neighbor interactions, open boundary conditions in both directions, and unperturbed Hamiltonian

$$H_0 := J \sum_{\langle i,j \rangle} \vec{s}_i \cdot \vec{s}_j . \quad (30)$$

(iv) The same square lattice model as in (30), but now with periodic boundary conditions in both directions. Similar to (1)-(3), an additional homogeneous magnetic field in z -direction is applied during time evolution in all four cases (i)-(iv). Accordingly, the spin ring without disorder represents an integrable model, whereas all the other examples (i), (iii), and (iv) are commonly considered as non-integrable, see also Sec. II A. Moreover, (ii) and (iv) are so-called translationally invariant models (see also Sec. IV below), while (i) and (iii) are not.

As our initial condition $\rho(0)$ (see above Eq. (9)) we choose a pure state of the form $\rho(0) = |\psi\rangle\langle\psi|$ with

$$|\psi\rangle \propto e^{-\frac{\beta}{2} \hat{H}} |\phi\rangle , \quad (31)$$

where $|\phi\rangle$ is a normalized random vector, which may be viewed as point on the unit sphere in $\mathbb{C}^{(2s+1)^\kappa}$, randomly sampled according to a uniform distribution. It is well-known that such an initial condition exhibits a so-called dynamical typicality property, meaning that it imitates

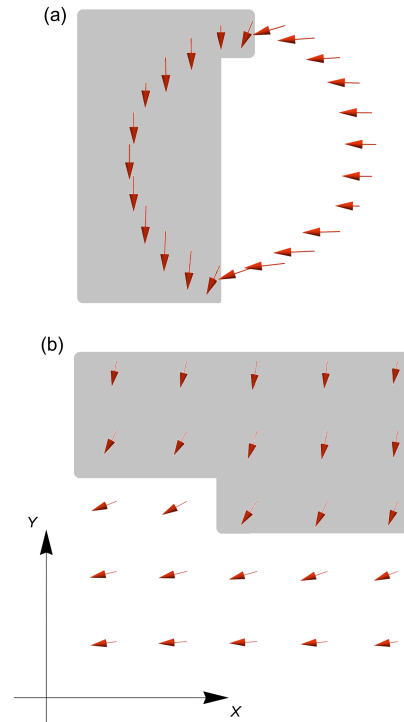


FIG. 1. Red arrows: Visualization of the projections to the (x, y) -plane of the expectation values of the local spin vector operators \vec{s}_i with respect to the initial state (31). (a): Spin ring models (i) and (ii) as specified around Eq. (29) and below (32). (b): Square lattice models (iii) and (iv) as specified around Eq. (30) and below (32). The grey and white regions indicate our choice of the sublattices Λ_1 and Λ_2 in (32). All the remaining model parameter values in (31) and (32) have been chosen in (a) as detailed in Fig. 2, and in (b) as detailed in Fig. 3.

very accurately the behavior of the canonical ensemble from (24), see, e.g. Ref. [41] and further references therein. More precisely speaking, for the vast majority of all those randomly sample initial states $\rho(0) = |\psi\rangle\langle\psi|$, the time-dependent expectation values in (9) become, for sufficiently large system sizes κ , practically indistinguishable from those which one would obtain by choosing $\rho(0)$ according to (24). A more precise analytical quantification of the remaining deviations is in general quite difficult, but we numerically verified that our results for different random initial states were indeed nearly indistinguishable on the scale of the subsequent plots. Apart from this connection to the canonical ensemble in (24), our initial state (31) represents, of course, already in itself a perfectly legitimate, generally far from equilibrium initial condition.

Once the initial state has been chosen, we numerically evolved it in time by means of Suzuki-Trotter product expansion techniques, as detailed, for instance, in Ref. [42].

While this temporal evolution is governed by the above

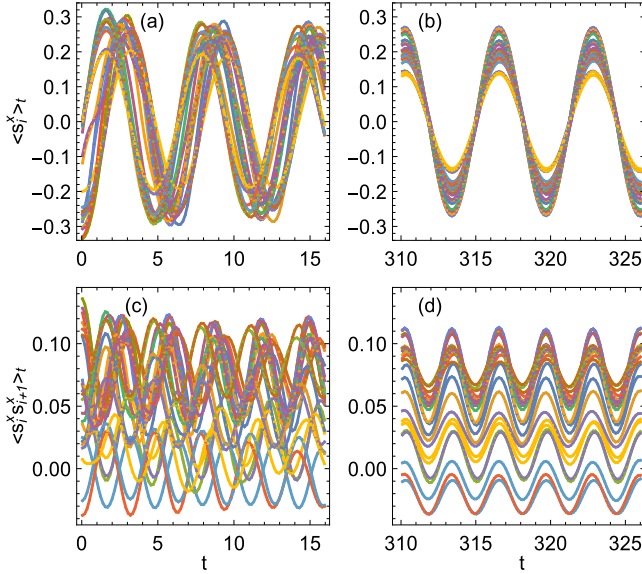


FIG. 2. (a) and (b): Expectation values (9) of the local observables $A = s_i^x$ for early times (a) as well as for late times (b) by numerically solving the spin ring model from (29) with $\kappa = 24$ spins, periodic boundary conditions, random couplings $J_i \in [-3, 1]$, and magnetic field $h = 1$, see also Eqs. (1)-(3). The different colors correspond to the 24 different observables $A = s_i^x$. The initial condition $\rho(0)$ is given by a canonical ensemble of the form (24), (25) with $\beta = 1$, choosing the Hamiltonian \tilde{H} according to (32) with $\tilde{H}_0 = H_0$, $h_x = h_y = 1$, and sublattices $\Lambda_{1,2}$ as indicated in Fig. 1(a), see also main text for more details. In the actual numerics, the behavior of the corresponding time evolved $\rho(t)$ was imitated by numerically evolving a random initial state as explained around Eq. (31). (c) and (d): Same, but for the observables $A = s_i^x s_{i+1}^x$ with $i = 1, \dots, 23$.

specified, so-called post-quench Hamiltonian H (see also Sec. III C), the so-called pre-quench Hamiltonian \tilde{H} , governing the initial condition via (24) and (31), is chosen as

$$\tilde{H} := \tilde{H}_0 + h_x \sum_{i \in \Lambda_1} s_i^x + h_y \sum_{i \in \Lambda_2} s_i^y, \quad (32)$$

where \tilde{H}_0 is of the same general structure as in (29) in our one-dimensional examples (i) and (ii), and as in (30) in our two-dimensional examples (iii) and (iv). More precisely speaking, \tilde{H}_0 was chosen identical to H_0 from (29) and (30) in (i) and (iii), respectively, while the same \tilde{H}_0 's as in (i) and (iii) were then also employed in (ii) and (iv), respectively. Furthermore, Λ_1 and $\Lambda_2 := \Lambda \setminus \Lambda_1$ in (32) denote two complementary subsets of the respective total lattices Λ (see above Eq. (1)). Their specific choice for the examples (i) and (ii) is visualized by the grey and white regions in Fig. 1(a), and for the examples (iii) and (iv) in Fig. 1(b). According to (32), the spins in those two sublattices (grey and white) are thus polarized by the external magnetic fields h_x and h_y along orthogonal

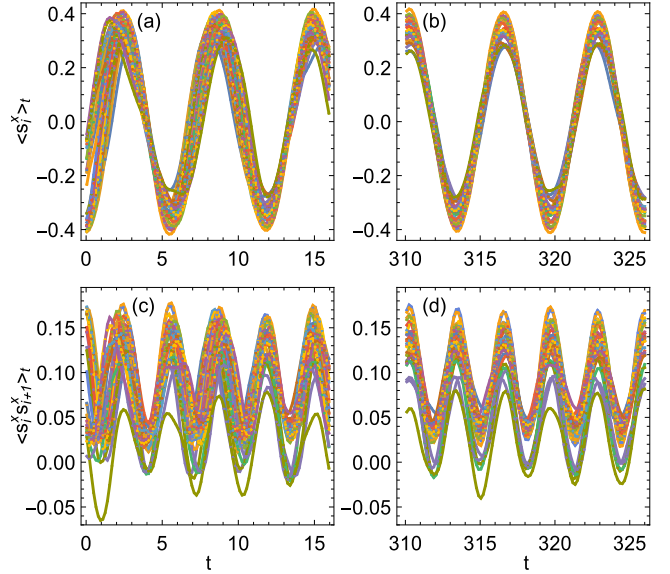


FIG. 3. Same as in Fig. 2, but now for a 5×5 square lattice model of the form (30) with $\kappa = 25$ spins, open boundary conditions, and couplings $J = -2$. In particular, the initial condition is again of the form (24), (25), (32) with $\beta = 1$, $\tilde{H}_0 = H_0$, and sublattices $\Lambda_{1,2}$ as indicated in Fig. 1(b).

directions, resulting via (31) in initial conditions for the individual spins as cartooned by the red arrows in Fig. 1.

Such inhomogeneous initial states with two extended domains of macroscopic magnetization appeared to us as particularly interesting and non-trivial examples. For instance, they clearly are *not* translationally invariant (see also Sec. IV below). Moreover, they are far from thermal equilibrium with respect to the post-quench Hamiltonian H .

As a first example, Fig. 2 displays the dynamics of various local observables for a spin ring model of type (i) with parameters given in the caption. With these parameters, the energy is not close to the edges of the spectrum. At early times, panels (a) and (c), the different observables behave rather irregularly, starting from their various initial values, whereas at later times, panels (b) and (d), all observables exhibit quite regular oscillations with angular frequency h in (b) and $2h$ in (d), thus confirming and illustrating our main analytical prediction from the previous subsections. The phases between these long-time oscillations seem to be astonishingly small, but the amplitudes differ quite notably (and in (d) also the time-averaged values). We will briefly return to this observation at the end of Sec. IV.

For the two-dimensional square lattice model of type (iii), qualitatively quite similar results are observed in Fig. 3. The main difference is that some of the long-time oscillations, especially in (d), still exhibit notable deviations from a strictly periodic behavior, which can be naturally understood as finite-size corrections to our analytical predictions. A more detailed discussion of these

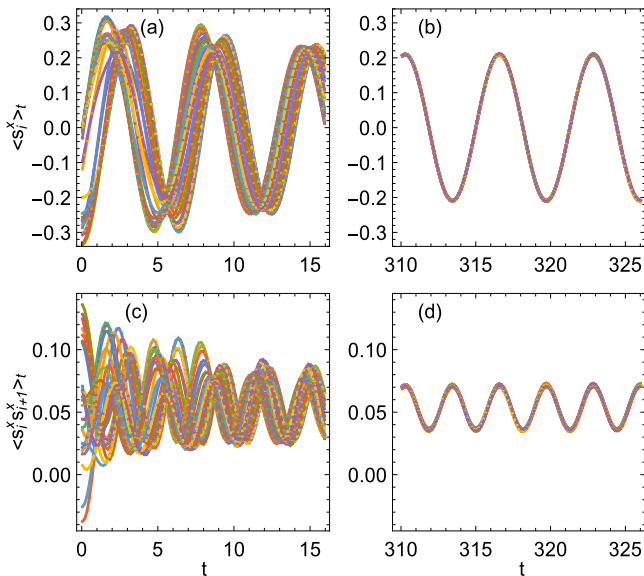


FIG. 4. Same as in Fig. 2, but now for non-random couplings $J_i = -1$ in the spin ring model (29). In particular, exactly the same the initial condition as in Fig. 2 was utilized.

finite-size effects is provided in Appendix B.

Turning to the two remaining, translationally invariant models (ii) and (iv), we encounter almost perfect synchronization of the individual local observables after initial transients have died out. Figure 4 displays this behavior for the spin ring model (ii), where local spin operators are related to each other by a translation along the ring, a symmetry operation under which the Hamiltonian is invariant, see also Sec. IV below. For late times, panels (b) and (d), the various oscillations superimpose perfectly, although the initial state is exactly the same as the one in Fig. 2, i.e. adapted to the Hamiltonian with disorder. We have verified that this synchronization behavior is practically independent of the initial conditions.

A qualitative similar behavior is also observed for our 5×5 square lattice model (iv) in Fig. 5. As will be explained in more detail in Sec. IV, the observed synchronization at large times has its origin in the model's translational invariance. Similarly as in Fig. 3, the remnant deviations from perfect synchronization, especially in Fig. 5(d), can be explained in terms of finite-size effects. Apparently, the fact that our square lattice models (iii) and (iv) only exhibit a relatively short period of 5 along each spatial direction is responsible for the stronger finite-size corrections in comparison to the spin ring models (i) and (ii). Similarly as in Appendix B, we also confirmed this expectation by directly comparing the numerical results for different system sizes with each other (not shown).

Further numerical examples for a variety of other model Hamiltonians and, more importantly, other initial conditions can also be found in Ref. [29].

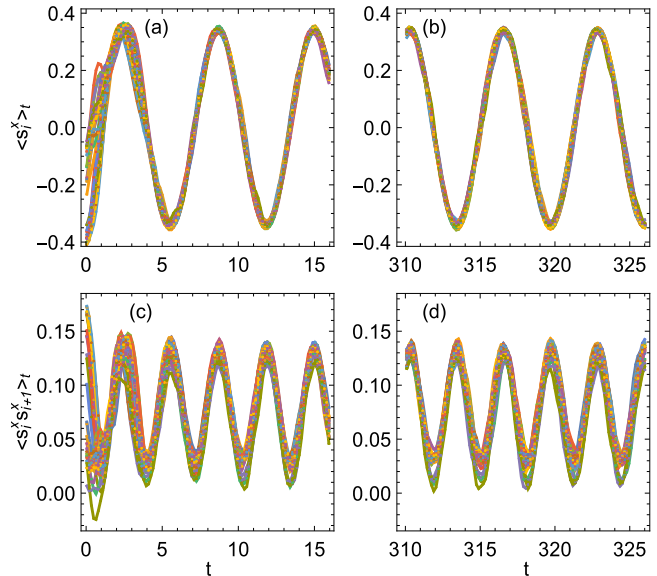


FIG. 5. Same as in Fig. 3, but now for periodic boundary conditions in the 5×5 square lattice model (30). In particular, exactly the same initial condition as in Fig. 3 was utilized.

IV. SYNCHRONIZATION

A particularly remarkable feature of the numerical results in Figs. 4 and 5 is the close agreement of all the differently colored graphs for sufficiently late times (right panels), while Figs. 2 and 3 do *not* exhibit such a behavior. In the following, our main objective is a better understanding of this numerical observation.

For the sake of simplicity, we mainly focus on one-dimensional spin models (2). Moreover, we require that the model is translationally invariant in the sense that site $i = \kappa + 1$ is identified with $i = 1$ (periodic boundary conditions) and the couplings J_{ij} only depend on the difference $i - j$ modulo κ . Finally, we restrict ourselves to the generic case that all energies E_n^0 are pairwise different, hence the quantities \bar{f}_ν are given by (17), see also the remarks below Eqs. (6) and (17).

For the rest, short- as well as long-range interactions are still admitted. Moreover, various generalizations, e.g., to higher-dimensional hypercubic lattices (with periodic boundary conditions) are straightforward, see also Sec. II A, but will not be explicitly worked out.

Denoting by \mathcal{T} the so-called translation operator, it is shown in Appendix C that

$$\langle n, l | \mathcal{T}^\dagger B \mathcal{T} | n, l' \rangle = \langle n, l | B | n, l' \rangle \quad (33)$$

for arbitrary Hermitian operators B and indices n, l, l' . Physically, $\mathcal{T}^\dagger B \mathcal{T}$ represents the same observable as B , except that “everything is shifted” by one unit along the periodic spin chain. For instance, for a single-site spin operator s_i^a (with $a \in \{x, y, z\}$) one finds that $\mathcal{T}^\dagger s_i^a \mathcal{T} = s_{i+1}^a$, and analogously for arbitrary sums and products of

such operators. In particular, the total spin components from (1) and the Hamiltonian from (2) are found to be translationally invariant in the sense that they commute with \mathcal{T} .

Taking into account (12) and (33), one can conclude that the quantities \bar{f}_ν in (17) and thus the function \mathcal{A}_t in (15) and (26) remain unchanged if we replace the observable A by its shifted counterpart $\mathcal{T}^\dagger A \mathcal{T}$. For instance, the expectation values of the single-site spin operators s_i^a are thus predicted to synchronize (look the same for all i) in the long run, and likewise for arbitrary sums and products of such operators. These findings are illustrated by Figs. 4 and 5, see also Sec. III E. The small remnant deviations from strict synchronizations in these numerical examples can be naturally understood as finite-size effects, see also Appendix B.

It readily follows that so-called local operators A_i with the property $\mathcal{T}^\dagger A_i \mathcal{T} = A_{i+1}$ will synchronize in the above sense not only with each other but also with their “intensive” counterpart $A := \sum_{i \in \Lambda} A_i / \kappa$, as exemplified by Eq. (34) below. We also remark that all these conclusions apply to arbitrary initial states $\rho(0)$ (as long as they satisfy (21)). In particular, $\rho(0)$ is *not* required to be translationally invariant.

An analogous line of reasoning implies that the initial condition $\rho(0)$ and its shifted counterpart $\mathcal{T}^\dagger \rho(0) \mathcal{T}$ exhibit in the long run (nearly) identical expectation values for arbitrary observables A and any initial state $\rho(0)$ which satisfies (21).

Altogether, the generically occurring, permanent long-time oscillations from Sec. III D are thus found to synchronize in the sense of being invariant under arbitrary translations of the considered observable, provided the system Hamiltonian (but not necessarily the initial condition) is translationally invariant.

Closely related numerical findings have been recently reported in Ref. [29]. Our present work amounts to a rigorous analytical validation and generalization of this numerical discovery of synchronization in closed systems of the form (1)-(3). Similarities and differences with respect to related synchronization phenomena in *open* systems have also been addressed already in Ref. [29] (see also [43]), and are therefore not repeated here. The salient point is that while the observable phenomena are similar, the basic physical mechanisms as well as the analytical methods are entirely different for closed and open systems.

Various slightly different notions of synchronization are reviewed, for instance, in Ref. [43]. Our present notion appears to us particularly simple and natural.

Intuitively, and also on the basis of our above calculations, it seems reasonable to suspect that translational invariance, or equivalence of all spin sites in general, is not only sufficient but that it generically is even necessary for the occurrence of synchronization in our present sense. This expectation is further corroborated by the numerical examples in Figs. 2 and 3.

V. SIMPLE ANALYTICAL EXAMPLES

Of foremost interest are cases where \bar{f}_ν in (16) is non-zero at least for one $\nu \neq 0$, giving rise to non-equilibration in the form of permanent oscillations in (26). In general, the explicit evaluation of \bar{f}_ν in (16) is a quite demanding task. In the following, we focus on some particularly simple examples.

A. Single spins

To begin with, we illustrate the general idea by means of the observables

$$M_a := \frac{1}{\kappa} S^a = \frac{1}{\kappa} \sum_{i \in \Lambda} s_i^a, \quad (34)$$

see also Eq. (1), i.e., the M_a are essentially the magnetizations along the spatial direction $a \in \{x, y, z\}$. Employing the usual raising and lowering operators

$$S^\pm := S^x \pm iS^y \quad (35)$$

one readily recovers the relations (see also around Eqs. (4)-(6))

$$S^\pm |n, l\rangle = c_{n,l}^\pm |n, l \pm 1\rangle \quad (36)$$

$$c_{n,l}^\pm := \sqrt{L_n(L_n + 1) - l(l \pm 1)}. \quad (37)$$

Observing that Eqs. (13) and (14) are linear in A , the same equations must also apply to the non-Hermitian operator $A := S^+$ from (35). Exploiting (12) and (36), it follows that

$$A_{nm}^{k+\nu, k} = \delta_{n,m} \delta_{\nu,1} c_{n,k}^+, \quad (38)$$

where $\delta_{n,m}$ and $\delta_{\nu,1}$ are Kronecker deltas. Hence, we can conclude with Eqs. (14) and (16) that

$$f_\nu(t) = \bar{f}_\nu = \delta_{\nu,1} f_1(0) \quad (39)$$

and with Eq. (15) and (13) that $\mathcal{A}_t := \langle A \rangle_t = \langle A \rangle_0 e^{iht}$. By means of a similar line of reasoning for $A := S^-$ one thus arrives at

$$\mathcal{S}_t^\pm := \langle S^\pm \rangle_t = \langle S^\pm \rangle_0 e^{\pm iht}. \quad (40)$$

Since $S^x = (S^+ + S^-)/2$ and $S^y = (S^+ - S^-)/2i$ according to (35), we finally obtain for the magnetizations $M_{x,y}$ from (34) the result

$$\langle M_x \rangle_t = a_1 \cos(ht) - b_1 \sin(ht), \quad (41)$$

$$\langle M_y \rangle_t = b_1 \cos(ht) + a_1 \sin(ht) \quad (42)$$

$$a_1 := \langle M_x \rangle_0, \quad (43)$$

$$b_1 := \langle M_y \rangle_0. \quad (44)$$

i.e., these particular observables exhibit perfect harmonic oscillations for all times t and for any initial state $\rho(0)$

with a non-vanishing expectation value of M_x or of M_y . In the same way one finds that

$$\langle M_z \rangle_t = \langle M_z \rangle_0, \quad (45)$$

i.e., this particular observable is, as expected, always a conserved quantity.

Similarly as in the first equality in (40), one readily sees that for the three specific observables $A := M_a$ from above, the auxiliary functions \mathcal{A}_t happen to be exactly identical to the true expectation values $\langle A \rangle_t$ for all t . In other words, none of further preconditions on the energies E_n^0 , the system size κ , and the initial condition $\rho(0)$ from Sec. III B are actually needed in these specific examples.

In a next step, let us focus on systems which satisfy the preconditions for our main result in Sec. III B as well as the preconditions for synchronization as detailed at the beginning of Sec. IV. According to the discussion at the end of Sec. IV, we thus can conclude that the single-spin expectation values $\langle s_i^a \rangle_t$ behave for most sufficiently large times t very similarly to each other and thus to $\langle M_a \rangle_t$ (see Eq. (34)), symbolically indicated as

$$\langle s_i^a \rangle_t \rightsquigarrow \langle M_a \rangle_t, \quad (46)$$

where $a \in \{x, y, z\}$. In particular, for any given observable $A := s_i^x$, the corresponding auxiliary function \mathcal{A}_t takes the i -independent explicit form (41), and similarly for s_i^y and s_i^z . On the other hand, for short times t the expectation values $\langle s_i^a \rangle_t$ are in general no longer close to $\langle M_a \rangle_t$. Rather, and as can be seen in Figs. 4 and 5, any given $\langle s_i^a \rangle_t$ generically exhibits a non-trivial initial relaxation process of its own, whose details depend in a complicated manner on the initial state $\rho(0)$ and on the Hamiltonian H . Moreover, even for large times t there will generically remain fluctuations of $\langle s_i^a \rangle_t$ about $\langle M_a \rangle_t$, which are negligibly small for most t but may become large for some very rare t 's (quantum recurrences or revivals [13]).

B. Higher harmonics

Our next examples are observables of the form $A := M_a^2$. By means of similar calculations as before one finds that

$$\langle M_x^2 \rangle_t = a_2 \cos(2ht) - b_2 \sin(2ht) + c_2, \quad (47)$$

$$\langle M_y^2 \rangle_t = -a_2 \cos(2ht) + b_2 \sin(2ht) + c_2, \quad (48)$$

$$\langle M_z^2 \rangle_t = \langle M_z^2 \rangle_0, \quad (49)$$

where we introduced the abbreviations

$$a_2 := \langle M_x^2 - M_y^2 \rangle_0 / 2, \quad (50)$$

$$b_2 := \langle M_x M_y + M_y M_x \rangle_0 / 2. \quad (51)$$

$$c_2 := \langle M_x^2 + M_y^2 \rangle_0 / 2, \quad (52)$$

As expected, $M_x^2 + M_y^2$ and M_z^2 are thus conserved quantities. Moreover, the observables $M_{x,y}^2$ exhibit perfect

harmonic oscillations for all t and for all initial conditions $\rho(0)$ with a non-vanishing expectation value in (49) or in (51). Last but not least, the oscillation frequency is now twice as large as in (41) and (42) (higher harmonics).

Combining (41) and (47) one can conclude that

$$\langle M_x^2 \rangle_t - \langle M_x \rangle_t^2 = a'_2 \cos(2ht) - b'_2 \sin(2ht) + c'_2, \quad (53)$$

$$a'_2 := (\sigma_{xx}^2 - \sigma_{yy}^2) / 2, \quad (54)$$

$$b'_2 := (\sigma_{xy}^2 + \sigma_{yx}^2) / 2, \quad (55)$$

$$c'_2 := (\sigma_{xx}^2 + \sigma_{yy}^2) / 2, \quad (56)$$

where

$$\sigma_{ab}^2 := \langle M_a M_b \rangle_0 - \langle M_a \rangle_0 \langle M_b \rangle_0 \quad (57)$$

for arbitrary $a, b \in \{x, y, z\}$. Analogous results as for M_x in (53) apply to M_y and M_z .

Incidentally, for observables of the form $s_i^x s_j^x$ one still can deduce from (5) and (16) that the long-time asymptotics must be of the general structure

$$\langle s_i^x s_j^x \rangle_t \rightsquigarrow a_{ij} \cos(2ht) + b_{ij} \sin(2ht) + c_{ij}. \quad (58)$$

Most importantly, the oscillation frequency is again twice as large as in (41), (46), in accordance with the numerical examples in Figs. 2-5. Similarly as in Eqs. (41)-(46), the coefficients a_{ij}, b_{ij}, c_{ij} in (58) are once more independent of h , but now their quantitative dependence on the initial state $\rho(0)$ and on the Hamiltonian H_0 is very difficult to specify in more detail. Analogous statements apply to observables of the form $s_i^a s_j^b$ with $a, b \in \{x, y\}$ and to products of more than two such factors.

C. Thermodynamic limit

Next we turn to the issue of how the above findings depend on the system size κ , and, in particular, how they behave for asymptotically large κ , i.e. in the thermodynamic limit. As usual in this context, we focus on systems whose size can be “upscaled” in a physically natural way. Particularly simple examples are translationally invariant Hamiltonians (see Sec. IV) with short-range interactions, i.e., the couplings J_{ij} in (3) decay sufficiently fast (and independent of κ) with increasing distance between the two sites i and j . Similarly, the initial states $\rho(0)$ must be chosen so that they amount to “physically similar situations” for different system sizes κ . For example, the system energy $\text{Tr}\{\rho(0)H\}$ is often expected to grow linearly with the system size κ , i.e., the energy density (energy per degree of freedom) is kept constant. Simple examples are canonical ensembles of the form (24), (25) with fixed parameters β and \vec{h}_i (independent of κ and i).

Rather than trying to formally define this class of “extensive” Hamiltonians H and initial states $\rho(0)$ more precisely, we assume as a “minimal requirement” that the concomitant expectation values of “intensive observables”, such as the magnetization M_a in (34), can be considered as asymptotically independent of the system size

κ , and that their statistical fluctuations and/or quantum uncertainties, as exemplified by (57), decay to zero with increasing system size κ (usually as $1/\kappa$). Moreover, we assume that correlations between local observables in the initial state $\rho(0)$, such as

$$c_{ij}^{ab} := \langle s_i^a s_j^b \rangle_0 - \langle s_i^a \rangle_0 \langle s_j^b \rangle_0, \quad (59)$$

decay to zero with the distance between the sites i and j sufficiently fast and asymptotically independently of the system size κ . Essentially, this assumption is tantamount to the so-called cluster decomposition property [44–48]. Though this property has until now only been rigorously established for a quite restricted set of examples [49–53], it is commonly expected to be obeyed by any “physically realistic” $\rho(0)$ – at least outside the realm where phase transitions may occur.

In particular, for systems that possibly may exhibit large thermal fluctuations as a precursor of spontaneous symmetry breaking in the thermodynamic limit, the energy density must be chosen outside the range where such effects occur. The opposite situation will be further explored in Sec. VI.

Given that the initial magnetizations $\langle M_a \rangle_0$ are asymptotically independent of the system size κ , the same follows for any later time t according to (41)–(45), and thus for the late-time behavior of any single spin according to (46).

In the same vein, the initial expectation values in (50)–(52) are expected to be asymptotically independent of the system size κ for physically realistic initial states $\rho(0)$, hence the same applies to the time-dependent expectation values in (47)–(49). On the other hand, the initial variances σ_{aa}^2 (see (57)) generically decay to zero for large κ . The same follows for the correlations σ_{ab}^2 in (57) upon observing that $[\sigma_{ab}^2]^2 \leq \sigma_{aa}^2 \sigma_{bb}^2$ (Cauchy-Schwarz inequality), and hence for the variance of M_x in (53), and similarly for M_y and M_z . Essentially, this reflects the common fact that quantum and statistical fluctuations become negligible for macroscopic observables. The main conclusion is that $\langle M_x^2 \rangle_t$ can often be very well approximated by $\langle M_x \rangle_t^2$.

Finally it is reasonable to expect that a large- κ asymptotics qualitatively similar to (46) will also apply to local observables of the form $s_i^a s_j^b$. However, more rigorous and/or quantitative statements along these lines are difficult to obtain, see also the discussion below Eq. (58).

On the other hand, quantum and statistical fluctuations of microscopic (local) observables are well-known to generically remain non-negligible. Accordingly, correlations at the initial time $t = 0$, as exemplified by (59), with not too large distances between the sites i and j , are not expected to approach zero for large κ , and likewise for the analogous correlations at any later time point t . Numerical examples in support of this expectation are provided by Figs. 2-5.

D. Final remarks

Our first remark is that in case of the macroscopic observables (34), the exact time-dependencies (41)–(45) can also be obtained “directly”, i.e., without exploiting our main results from Sec. III, and likewise for (47)–(52). Namely, by exploiting the specific symmetries of the Hamiltonian H in (2), the Heisenberg equations of motion which govern the expectation values of those observables can be readily solved, as detailed, e.g., in Ref [29]. From this viewpoint, the absence of equilibration in such models may thus be considered as a relatively obvious consequence of their special symmetry properties.

For most other observables, the generic occurrence of permanent long-time oscillations is a far from obvious key finding of our present work. The fact that this finding is indeed non-trivial is already quite evident by recalling that usually an (approximately) time-periodic behavior only appears after sufficiently long times (see Figs. 2-5), and even then the actual expectation values still exhibit certain deviations from strict periodicity (for systems of finite size). Moreover, the oscillations are asynchronous unless the system happens to be translationally invariant (Sec. IV).

Our second remark is that “single spin observables” s_i^a with $a \in \{x, y\}$ and their intensive counterparts M_a from (34) were found in Sec. V A to exhibit harmonic long-time oscillations with angular frequency h . In the same vein, “two-spin observables” $s_{i_1}^{a_1} s_{i_2}^{a_2}$ with $a_{1,2} \in \{x, y\}$ were found to harmonically oscillate with angular frequency $2h$ in Sec. V B, while $\langle M_a^2 \rangle_t$ turned out to be often close to $\langle M_a \rangle_t^2$ in Sec. V C. Analogously, it is quite evident that harmonic oscillations with angular frequency νh will arise for ν -spin observables $s_{i_1}^{a_1} \cdots s_{i_\nu}^{a_\nu}$, while $\langle M_a^\nu \rangle_t$ will be close to $\langle M_a \rangle_t^\nu$ in many cases. The latter example implies that the long-time oscillations are in general *not* of a purely harmonic character.

VI. EQUILIBRIUM CORRELATIONS AND TIME CRYSTALS

Throughout this section we restrict ourselves to system states of the specific form

$$\rho = \sum_{nl} p_{nl} |n, l\rangle \langle n, l| \quad (60)$$

with $p_{nl} \geq 0$ and $\sum_{nl} p_{nl} = 1$. It follows from (7) that $[H, \rho] = 0$, i.e. the state ρ remains unchanged in the course of time (steady or equilibrium state). Particularly important examples are thermal equilibrium ensembles of the canonical form

$$\rho = e^{-\beta H} / \text{Tr}\{e^{-\beta H}\}. \quad (61)$$

Other examples are microcanonical ensembles, or, more generally, largely arbitrary diagonal ensembles of low purity, see also Eqs. (23), (27), and below Eq. (66).

In other words, we are dealing here with the exceptional cases announced below Eq. (26), for which any permanent oscillations are strictly ruled out. Our main objective in this section is to show that the basic SU(2) symmetry (see above Eq. (4)), which is at the origin of the permanent oscillations in the generic case, still gives rise to some different kind of interesting properties in our present exceptional cases, including systems at thermal equilibrium as particularly prominent examples. In order to achieve this goal, the salient point will be to consider so-called temporal correlations (see Eq. (62) below) instead of the so-far employed expectation values (see Eq. (9)). Incidentally, these explorations will at the same time very naturally open up a connection to the topic of time crystals, which recently attracted a considerable amount of attention.

As announced, the quantities of foremost interest throughout the present section will be temporal correlations, also called, among others, dynamic or two-point correlation functions, and being formally defined as

$$C_{AB}(t) := \text{Tr}\{\rho AB(t)\} \quad (62)$$

for any given pair of observables A and B , where $B(t) := e^{iHt} B e^{-iHt}$ (Heisenberg picture, $\hbar = 1$).

Similarly as in (10)-(14) one finds that

$$C_{AB}(t) = \sum_{\nu} g_{\nu}(t) e^{i\nu ht}, \quad (63)$$

$$g_{\nu}(t) := \sum_{mn} e^{i(E_n^0 - E_m^0)t} \sum_k p_{mk} A_{mn}^{k,k+\nu} B_{nm}^{k+\nu,k}, \quad (64)$$

and similarly as in (15), (16), (22) that

$$C_{AB}(t) \rightsquigarrow \sum_{\nu} \bar{g}_{\nu} e^{i\nu ht}, \quad (65)$$

$$\bar{g}_{\nu} := \sum'_{mnk} p_{mk} A_{mn}^{k,k+\nu} B_{nm}^{k+\nu,k} \quad (66)$$

under the very same preconditions as those discussed in Secs. III B and III C. The detailed derivation is quite similar to Appendix A – see also Supplemental Material of Ref. [30] – and therefore omitted here.

As a consequence, the generic appearance of permanent oscillations is predicted similarly as in Sec. III D, and of synchronization effects similarly as in Sec. IV in case of translationally invariant systems. In particular, correlations of local observables A_i and B_i with the property $\mathcal{T}^\dagger A_i \mathcal{T} = A_{i+1}$ and $\mathcal{T}^\dagger B_i \mathcal{T} = B_{i+1}$ are predicted to synchronize with each other, and also with the correlations of their intensive counterparts $A := \sum_{i \in \Lambda} A_i / \kappa$ and $B := \sum_{i \in \Lambda} B_i / \kappa$, respectively.

Note that the correlation in (62) is, in general, a complex valued function of t , and as such not an immediately observable quantity. However, analogous predictions readily carry over to its real (symmetrized) part

$$C_{AB}^s(t) := [\text{Tr}\{\rho AB(t)\} + \text{Tr}\{\rho B(t)A\}]/2, \quad (67)$$

and analogously for its imaginary part.

Focusing on the specific observables $A = B = M_x$ from (34), one finally finds, similarly as in Sec. V, for arbitrary t and without any further approximation that

$$C_{M_x M_x}^s(t) = \tilde{a}_2 \cos(ht), \quad (68)$$

$$\tilde{a}_2 := \text{Tr}\{\rho M_x^2\}, \quad (69)$$

and likewise for $A = B = M_y$. In case of a translationally invariant system, we furthermore can conclude under similar conditions as above (46) that

$$C_{s_i^x s_i^x}^s(t) \rightsquigarrow C_{M_x M_x}^s(t). \quad (70)$$

These findings imply interesting conclusions with respect to the topic of time crystals. At the focus of the latter issue are, generally speaking, various conceivable forms and disguises of a spontaneously broken time-translation symmetry, see, e.g., Refs. [23, 24] for recent reviews. Here, we specifically address the possible occurrence of such fascinating phenomena in *isolated* many-body quantum systems *at thermal equilibrium*, meaning that no periodic driving and no external bath(s) or other sources of dissipation are involved, nor do we focus on the zero temperature limit or ground state properties, nor is the thermodynamic limit taken before the long-time limit [23, 24]. Under these circumstances, a particularly well-established definition of a time crystal explicitly refers to the behavior of temporal correlations at thermal equilibrium, requiring that they must exhibit permanent oscillations in time as well as long-range order in space [26]. In our present context, this is largely equivalent [26–28] to the requirement that there must exist intensive observables A, B , as exemplified by (34) and more generally defined below Eq. (66), whose correlation function in (62) exhibits permanent oscillations that do not tend to zero for asymptotically large system size κ , see below (59).

Combining this definition and Eq. (68), a time crystal will thus be realized by focusing on the example $A = B = M_x$ and showing that \tilde{a}_2 in (69) approaches a positive limiting value for asymptotically large κ in the canonical ensemble from (61). Observing (69) and that $\text{Tr}\{\rho M_x\} = 0$ such a behavior of \tilde{a}_2 is tantamount to the appearance of macroscopic thermal fluctuations of M_x and is thus expected to arise if the Heisenberg model in (1)-(3) exhibits in the thermodynamic limit a spontaneous symmetry breaking (phase transition) with respect to M_x . In this context it may be worth to recall that, as always, we tacitly focus on cases with a non-vanishing external field h in (2).

Remarkably, we thus established a direct connection between a spontaneously broken time-translation invariance in the context of time crystals, and a spontaneously broken spatial symmetry in the context of phase transitions at thermal equilibrium.

As demonstrated analytically in Refs. [26–28], this kind of time crystal is in fact impossible, at least for all many-body systems with short-range interactions. Accordingly,

also the above-mentioned phase transition can be ruled out.

An alternative, weaker definition of a time crystal has recently been proposed and explored in Ref. [25], requiring that the ratio between the temporal correlation in (62) and its initial value $C_{AB}(0)$ must exhibit permanent long-time oscillations. According to (68), this condition is always fulfilled for the specific choice $A = B = M_x$. In other words, according to this definition, a time crystal is expected to generically arise for any model of the general form (1)-(3) with non-vanishing field h . Similarly to the discussion at the end of Sec. III D, our present findings thus complement and substantially extend those obtained in the seminal previous Ref. [25].

VII. SUMMARY AND CONCLUSIONS

Our first main prediction, see Sec. III, is that any Heisenberg model of the general form (1)-(3) gives rise to time-dependent expectation values (9), which become practically indistinguishable from the auxiliary function (26) for practically all sufficiently large times t . The very weak preconditions for this prediction are that the system size κ must be large, the maximal gap degeneracy γ^0 must not be exceedingly large, see below Eq. (21), and the maximal level population p_{\max} must be small, see Eq. (21). For instance, the latter condition is known to be fulfilled if the initial state arises as the result of a canonical quench, see Sec. III C.

In turn, this auxiliary function (26) generically exhibits time-periodic but not necessarily harmonic oscillations, hence the same must be (approximately) the case for the long-time behavior of the corresponding expectation values in (9), as exemplified by Figs. 2-5. The main requirements for such permanent long-time oscillations are a non-vanishing magnetic field h in (2), and a non-equilibrium initial condition (thus excluding diagonal ensembles of the form (27) or (60)). In particular, the system does not exhibit equilibration in all these cases.

As detailed at the end of Sec. III B, the absence of equilibration can be traced back to the existence of highly degenerate energy gaps, which in turn may be viewed as a consequence of the spatially homogeneous external field and the SU(2) symmetry of the field-free model. On the other hand, whether or not the system satisfies the so-called eigenstate thermalization hypothesis [2-4] does not seem to play a major role.

We remark that the considered models (1)-(3) themselves are not subject to any time-dependent external driving. Moreover, all the above findings are independent of whether the system is integrable or not, features disorder and possibly many-body localization or not, is extensive due to short-range interactions or not, nor does the dimensionality of the system play any significant role.

Put differently, approximately periodic long-time oscillations are predicted to occur for almost any observable. Moreover, during some initial time interval, the expect-

ation values are generically far from being periodic, and exhibit some small deviations from strict periodicity even for large times. Finally, those oscillations are in general not of a purely harmonic character, including as special cases oscillations with arbitrary multiples of the reference frequency h , cf. Eq. (26). As discussed in Sec. V D, for such observables we are thus unable to complement our analytical theory by some simple “physical explanation” of what is essentially going on.

Another challenging open problem is to explain all observable properties for a finite magnetic field h in (2) in terms of the field-free properties. More precisely speaking, the eigenvalues and eigenvectors are of course trivially related via (7), (8), but does the behavior of all physically relevant observables for $h = 0$ already determine their behavior for $h \neq 0$? For instance, the idea to switch into some suitable rotating frame might appear very natural and promising at first glance. However, closer inspection reveals that for most observables the behavior for $h \neq 0$ cannot be deduced from that for $h = 0$ in this way.

Our second main result (see Sec. IV) is the prediction of synchronization under the additional requirement that the system is translationally invariant and thus obeys periodic boundary conditions in all spatial directions. Here, the term synchronization means that the above discussed long-time oscillations become approximately invariant under arbitrary translations of any given observable, as exemplified by Figs. 4 and 5. Once again, this approximate invariance is furthermore predicted to become asymptotically exact for large times and large system sizes. Even more generally speaking, and without any reference to some underlying lattice geometry, it seems in fact sufficient to require that all spins of the considered model are equivalent, and likewise for the synchronizing observables.

We emphasize that our present synchronization phenomenon does not depend on whether the interactions J_{ij} in (3) are negative (i.e. of ferromagnetic character) or not [29], contrary to what one might have naively expected to be necessary for the “alignment” of all the spins in such a system. In the same vein, the system’s dimensionality once again plays no role, nor is it necessary that the initial condition is translationally invariant. More generally speaking, ordering and phase transition phenomena at thermal equilibrium are apparently of little help to better understand our present synchronization effects, nor are we able to provide any other kind of simple intuitive explanation of the basic underlying physics.

Obviously, the above predicted long-time oscillations of any given observable A in general still depend in a very complicated way – via the phases and amplitudes in (26) – on the choice of the initial condition $\rho(0)$. However, for translationally invariant Hamiltonians those long-time oscillations were shown in Sec. IV to be invariant under arbitrary translations of the initial condition $\rho(0)$, even if $\rho(0)$ itself is not translationally invariant. This quite remarkable finding is in fact equivalent to the

prediction of synchronization, and therefore seems again not to admit a simple physical explanation.

Our third main result concerns the issue of time crystals. Unfortunately, even the precise definition of a time crystal still appears to be somewhat ambiguous. For instance, already our permanent oscillations from Sec. III can be considered as the characteristic signature of a time crystal according to one of the definitions provided in Ref. [24] (see Figure 8, second column, last row therein): Indeed, since the time-translation invariance of the model Hamiltonian is spontaneously broken and reduced to a time-discrete invariance for arbitrarily long times, which in turn may be viewed as a thermodynamic limit in the time domain, it seems justified [24] to speak of a “crystal” in the time domain. In our present explorations in Sec. VI, we mainly focused on the somewhat more generally established definition of a time crystal from Ref. [26]. We also may recall that the no-go theorem for this type of time crystals from Ref. [26] has been shown in Ref. [24] to still contain a loophole, which in turn has been subsequently closed in [27], compare also [28]. Our present explorations are of course compatible with this latter no-go theorem, i.e., we do not find a time crystal in the sense of Ref. [26]. Finally, yet another, somewhat weaker definition of a time crystal has been proposed in Ref. [25], according to which our findings in Sec. VI lead to the conclusion that models of the general form (1)-(3) generically do exhibit the characteristic signature of a time crystal. The question of what we actually gained by knowing whether or not some given model system qualifies as a time crystal in one or the other sense remains unclear to the present authors.

Finally, it seems reasonable to expect that our main findings will also be recovered in a broad class of alternative models such as the Hubbard model, as long as their general symmetry properties are similar as in our present model, i.e., analogous the SU(2) symmetry of our field-free model and to the spatial homogeneity of the externally applied field.

ACKNOWLEDGMENTS

This work was funded by the Deutsche Forschungsgemeinschaft (DFG, German Research Foundation) – 355031190 (FOR 2692), 397303734, and 397300368. We thank Heinz-Jürgen Schmidt for valuable suggestions and remarks. We acknowledge support for the publication costs by the Open Access Publication Fund of Bielefeld University and the Deutsche Forschungsgemeinschaft (DFG).

Appendix A: Derivation of Eq. (20)

As usual, the unperturbed energies are denoted by E_n^0 with $n \in \{1, \dots, N\}$ (see below (6)), and the operator

norm (largest eigenvalue in modulus) of any Hermitian operator A is denoted by $\|A\|$.

Choosing $l = L_n$ in (5), and exploiting that $\|S^z\| \leq \sum_{i \in \Lambda} \|s_i^z\| = \kappa s$, where s is the single-site spin quantum number and κ the system size (see above (1)), we can conclude that

$$L_n \leq \kappa s \quad (\text{A1})$$

for any $n \in \{1, \dots, N\}$.

Given that a single spin at any given site i spans a Hilbert space of dimension $2s+1$, the dimensionality of the full Hilbert space will be $(2s+1)^\kappa$. Hence, the total number N of all energy eigenvalues E_n^0 can be *upper bounded* by $(2s+1)^\kappa$,

$$N \leq (2s+1)^\kappa. \quad (\text{A2})$$

Conversely, for any given n , the total number $2L_n+1$ of all possible labels l (see below (6)) is upper bounded by $2\kappa s+1$ according to (A1). We thus obtain the *lower bound*

$$N \geq \frac{(2s+1)^\kappa}{2\kappa s+1}. \quad (\text{A3})$$

Altogether, (A2) and (A3) imply that the number N of energy eigenvalues E_n^0 must grow exponentially with the system size κ

The set of all possible (ordered) pairs of indices m and n is defined as

$$\mathcal{G}_{\text{tot}} := \{(m, n) \mid m, n \in \{1, \dots, N\}\}. \quad (\text{A4})$$

For any given pair $\alpha = (m, n) \in \mathcal{G}_{\text{tot}}$ we furthermore define

$$G_\alpha := E_n^0 - E_m^0, \quad (\text{A5})$$

$$\eta_\alpha^\nu := \sum_k \rho_{mn}^{k, k+\nu} A_{nm}^{k+\nu, k}. \quad (\text{A6})$$

Hence, (14) can be rewritten as

$$f_\nu(t) := \sum_{\alpha \in \mathcal{G}_{\text{tot}}} e^{iG_\alpha t} \eta_\alpha^\nu. \quad (\text{A7})$$

Next, we introduce the subset $\mathcal{G} \subset \mathcal{G}_{\text{tot}}$ of all pairs (m, n) with the property that $E_m^0 \neq E_n^0$, i.e.,

$$\mathcal{G} := \{\alpha \in \mathcal{G}_{\text{tot}} \mid G_\alpha \neq 0\}. \quad (\text{A8})$$

Accordingly, its complement satisfies

$$\bar{\mathcal{G}} := \mathcal{G}_{\text{tot}} \setminus \mathcal{G} = \{\alpha \in \mathcal{G}_{\text{tot}} \mid G_\alpha = 0\}. \quad (\text{A9})$$

It readily follows that the maximal gap degeneracy from (19) can be rewritten in the form

$$\gamma^0 = \max_{\beta \in \bar{\mathcal{G}}} |\{\alpha \in \mathcal{G} \mid G_\alpha = G_\beta\}|, \quad (\text{A10})$$

where $|S|$ denotes the number of elements contained in the set S . Similarly, the long-time average of $f_\nu(t)$ from (14) or (A7) can be rewritten in the form (16) or

$$\bar{f}_\nu = \sum_{\alpha \in \mathcal{G}} \eta_\alpha^\nu, \quad (\text{A11})$$

respectively.

As announced in the main text, our objective is to show that the difference

$$\Delta(t) := \langle A \rangle_t - \mathcal{A}_t \quad (\text{A12})$$

between the time-dependent expectation values from (13) and the auxiliary function from (15) is small for most sufficiently late times t . Employing (13), (15), (A7), (A9), and (A11), we therefore rewrite (A12) as

$$\Delta(t) = \sum_\nu \delta_\nu(t) e^{i\nu ht}, \quad (\text{A13})$$

$$\delta_\nu(t) := f_\nu(t) - \bar{f}_\nu = \sum_{\alpha \in \mathcal{G}} e^{iG_\alpha t} \eta_\alpha^\nu. \quad (\text{A14})$$

Next we recall that the sum over the indices m, n, k, l in (10) is tacitly restricted to pairs n, l for which $|n, l\rangle$ are well-defined eigenvectors in (7), i.e. $n \in \{1, \dots, N\}$ and $l \in \{-L_n, \dots, L_n\}$, and likewise for the pairs m, k . Alternatively, for indices n, l so that $|n, l\rangle$ is not a well-defined eigenvector, we may define those (so far undefined) vectors $|n, l\rangle$ as being equal to the null vector (hence $\rho_{mn}^{k,l} = 0$, $A_{nm}^{l,k} = 0$). As a consequence, we may now consider all four indices m, n, k, l in the sum in (10) to run over all integer values, and likewise for the summation indices in (14), (16), and (A6). Furthermore, it follows that the matrix elements $\rho_{mn}^{k,k+\nu}$ are zero if $k \notin \{-L_m, \dots, L_m\}$ or $k + \nu \notin \{-L_n, \dots, L_n\}$. Hence, it is sufficient to keep on the right-hand side in (A6) only those summands which satisfy $|k| \leq L_m$ and $|\nu + k| \leq L_n$. Observing (A1) and $|\nu + k| \geq |\nu| - |k|$ (triangle inequality) it follows that $|\nu| - \kappa s \leq |\nu| - |k| \leq |\nu + k| \leq \kappa s$ must be fulfilled. As a consequence, it is necessary that $|\nu| \leq 2\kappa s$ in order that η_α^ν in (A6) is non-zero. Therefore, it is sufficient to keep in (A13) only those ν which are contained in $I := \{-2\kappa s, \dots, 2\kappa s\}$, and by employing the Cauchy-Schwarz inequality we obtain

$$|\Delta(t)|^2 \leq \sum_{\nu \in I} |\delta_\nu(t)|^2 \sum_{\nu \in I} |e^{i\nu ht}|^2. \quad (\text{A15})$$

The last sum can be identified with $4\kappa s + 1$, yielding

$$|\Delta(t)|^2 \leq (4\kappa s + 1) \sum_\nu |\delta_\nu(t)|^2, \quad (\text{A16})$$

where, without loss of generality, the sum has again been extended to all integer indices ν .

Denoting, as in the main text, the temporal average of an arbitrary function $f(t)$ over the time interval $[0, T]$ by

$$\langle f(t) \rangle_T := \frac{1}{T} \int_0^T dt f(t), \quad (\text{A17})$$

we can conclude from (A14) that

$$\langle |\delta_\nu(t)|^2 \rangle_T = \sum_{\alpha, \beta \in \mathcal{G}} (\eta_\alpha^\nu)^* M_T^{\alpha\beta} \eta_\beta^\nu, \quad (\text{A18})$$

$$M_T^{\alpha\beta} := \left\langle e^{-i(G_\alpha - G_\beta)t} \right\rangle_T. \quad (\text{A19})$$

Viewing $M_T^{\alpha\beta}$ as the matrix elements of some operator M_T , one can infer from (A19) that M_T is Hermitian and non-negative, and therefore

$$\sum_{\alpha, \beta \in \mathcal{G}} (\eta_\alpha^\nu)^* M_T^{\alpha\beta} \eta_\beta^\nu \leq \|M_T\| \sum_{\alpha \in \mathcal{G}} |\eta_\alpha^\nu|^2. \quad (\text{A20})$$

As detailed, e.g., in Ref. [11], compare Eq. (14) therein, one can furthermore show that

$$\|M_T\| \leq 2\gamma^0 \quad (\text{A21})$$

for all sufficiently large T , where γ^0 is given in (A10).

Altogether, (A16), (A18), (A20), and (A21) thus imply

$$\langle |\Delta(t)|^2 \rangle_T \leq 2\gamma^0 (4\kappa s + 1) \sigma^2, \quad (\text{A22})$$

$$\sigma^2 := \sum_\nu \sum_{\alpha \in \mathcal{G}} |\eta_\alpha^\nu|^2, \quad (\text{A23})$$

for all sufficiently large T . Extending the sum in (A23) over all index pairs $\alpha \in \mathcal{G}_{\text{tot}}$ and exploiting (A6), we find

$$\begin{aligned} \sigma^2 &\leq \sum_\nu \sum_{mn} \sum_{kl} \rho_{mn}^{k,k+\nu} A_{nm}^{k+\nu,k} (\rho_{mn}^{l,l+\nu} A_{nm}^{l+\nu,l})^*, \\ &= \sum_{\nu mn} Q_{\nu mn}, \end{aligned} \quad (\text{A24})$$

$$Q_{\nu mn} := \sum_{kl} V_{\nu mn}^{k,l} (V_{\nu mn}^{l,k})^*, \quad (\text{A25})$$

$$V_{\nu mn}^{k,l} := \rho_{mn}^{k,k+\nu} (A_{nm}^{l+\nu,l})^*. \quad (\text{A26})$$

Utilizing the Cauchy-Schwarz inequality in (A25) implies

$$|Q_{\nu mn}|^2 \leq \sum_{kl} |V_{\nu mn}^{k,l}|^2 \sum_{kl} |V_{\nu mn}^{l,k}|^2. \quad (\text{A27})$$

Observing that the two sums on the right-hand side are in fact identical, we can infer with (A24) that

$$\sigma^2 \leq \sum_{\nu mn} |Q_{\nu mn}| \leq \sum_{\nu mnkl} |V_{\nu mn}^{k,l}|^2 \quad (\text{A28})$$

and with (A26) that

$$\sigma^2 \leq \sum_{\nu mnkl} |\rho_{mn}^{k,k+\nu}|^2 |A_{nm}^{l+\nu,l}|^2. \quad (\text{A29})$$

Exploiting (11) and the Cauchy-Schwarz inequality, one can conclude that $|\rho_{mn}^{k,l}|^2 \leq \rho_{mm}^{k,k} \rho_{nn}^{l,l}$. Since the density operator $\rho(0)$ must be semi-positive, it follows with (11) that $\rho_{mm}^{k,k}$ and $\rho_{nn}^{l,l}$ are non-negative, real numbers.

Altogether, $|\rho_{mn}^{k,k+\nu}|^2$ in (A29) can thus be upper bounded by $\rho_{mm}^{k,k} p_{\max}$, where p_{\max} is defined in (18), yielding

$$\sigma^2 \leq p_{\max} \sum_{mk} \rho_{mm}^{k,k} W_m, \quad (\text{A30})$$

$$W_m := \sum_l w_{ml}, \quad (\text{A31})$$

$$w_{ml} := \sum_{n\nu} |A_{nm}^{l+\nu,l}|^2. \quad (\text{A32})$$

Replacing in (A32) the summation index ν by $j := l + \nu$ and exploiting (12) thus yields

$$w_{ml} = \sum_{nj} |A_{nm}^{j,l}|^2 = \sum_{nj} \langle m, l | A | n, j \rangle \langle n, j | A | m, l \rangle. \quad (\text{A33})$$

Since $\sum_{nj} |n, j \rangle \langle n, j|$ is the unit operator, we see that w_{ml} equals $\langle m, l | A^2 | m, l \rangle$ and thus

$$W_m = \sum_l \langle m, l | A^2 | m, l \rangle. \quad (\text{A34})$$

As discussed below (A14), the summands on the right-hand side of (A34) are zero for $l \notin \{-L_m, \dots, L_m\}$. In other words, there are at most $2L_m + 1$ non-vanishing summands. Furthermore, each of those summands can be upper bounded by $\|A^2\| = \|A\|^2$. Due to (A1) we thus arrive at

$$W_m \leq (2\kappa s + 1) \|A\|^2. \quad (\text{A35})$$

Observing (11), the remaining sum in (A30) can be identified with $\text{Tr}\{\rho(0)\} = 1$, yielding

$$\sigma^2 \leq (2\kappa s + 1) \|A\|^2 p_{\max}. \quad (\text{A36})$$

Together with (A22), we finally can conclude that

$$\langle |\Delta(t)|^2 \rangle_T \leq 4\gamma^0 (2\kappa s + 1)^2 \|A\|^2 p_{\max} \quad (\text{A37})$$

for all sufficiently large T .

Note that if we replace A by $A + c$ then both terms on the right-hand side in (A12) are shifted by the same constant c , thus the left-hand side is independent of c . Accordingly, the left-hand side in (A37) is independent of c , while the right-hand side yields in general a different upper bound for different choices of c . Denoting by a_{\max} and a_{\min} the largest and smallest eigenvalues of A , respectively, one finds that the tightest upper bound is achieved for the choice $c = -(a_{\max} + a_{\min})/2$. Altogether, (A37) and (A12) thus yield

$$\langle [\langle A \rangle_t - \mathcal{A}_t]^2 \rangle_T \leq \gamma^0 (2\kappa s + 1)^2 \Delta_A^2 p_{\max} \quad (\text{A38})$$

for all sufficiently large T , where $\Delta_A := a_{\max} - a_{\min}$ is the measurement range of A (difference between largest and smallest possible measurement outcomes). In other words, we recover Eq. (20).

Appendix B: Finite-Size Effects

The numerical examples considered in Sec. III E deal with still relatively small spin systems. In particular, for the two-dimensional models with open boundary conditions one might wonder how strongly finite-size effects impact the theoretically predicted periodicity of time-dependent expectation values at late times. We also remind the reader that synchronization is not to be expected in such models with open boundary conditions since they are not translationally invariant.

In order to get an impression, Fig. 6 compares the late time behavior of spin-spin correlation functions for the already shown example of a 5×5 square lattice (see Fig. 3(d)) with the smaller counterpart of a 4×4 square lattice. As is obvious for the naked eye, the larger system displays much smaller deviations from periodicity than the smaller system. Unfortunately, numerical explorations of even larger square lattices are prohibited by the exponential growth of the underlying Hilbert space, but we think that already our present comparison provides sufficient evidence that for larger systems better and better periodicity is to be expected.

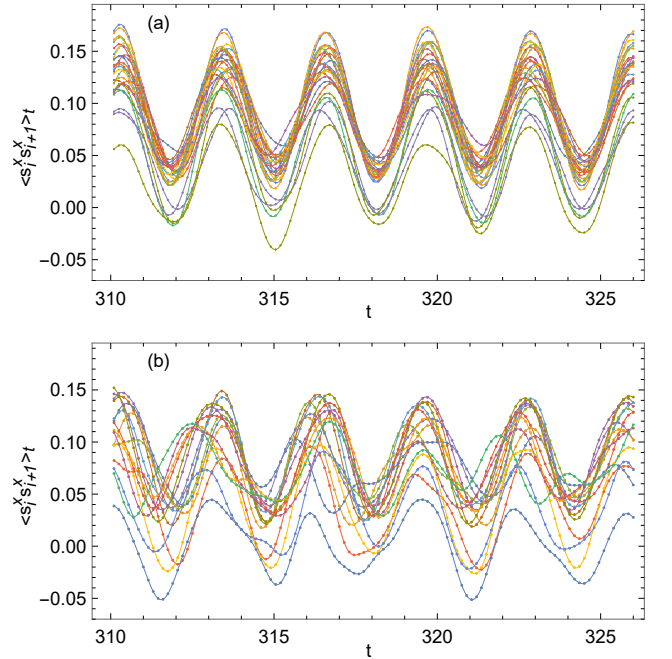


FIG. 6. (a) Same numerical data as in Fig. 3(d), i.e., for a 5×5 square lattice model with open boundary conditions. (b): Corresponding data for a 4×4 square lattice.

Appendix C: Derivation of Eq. (33)

We focus on spin models (2) on a *one-dimensional* lattice $\Lambda = \{1, \dots, \kappa\}$ with periodic boundary conditions. [Generalizations to hypercubic lattices in arbitrary di-

mensions are straightforward.] In other words, we are dealing with κ identical “units” (spins) on a ring (chain with periodic boundary conditions) which are labeled by $i \in \{1, \dots, \kappa\}$.

In the absence of interactions, each unit “lives” on a Hilbert space \mathcal{H}_i with orthonormal basis $|k\rangle_i$, where $k = 1, \dots, 2s+1$. Apart from “belonging” to different units i , all those Hilbert spaces are identical copies of each other.

The pertinent Hilbert space \mathcal{H} of the total system is the tensor product of all the \mathcal{H}_i . Abbreviating κ -tuples (k_1, \dots, k_κ) as \vec{k} , the vectors $|\vec{k}\rangle := |k_1\rangle_1 \cdots |k_\kappa\rangle_\kappa$ then amount to an orthonormal basis of \mathcal{H} .

Next, a “shift” or “translation” operator $\mathcal{T} : \mathcal{H} \rightarrow \mathcal{H}$ is defined via its action on any basis vector: $\mathcal{T}|\vec{k}\rangle := |k_2\rangle_1 |k_3\rangle_2 \cdots |k_\kappa\rangle_{\kappa-1} |k_1\rangle_\kappa$. One readily concludes that \mathcal{T} is norm-preserving. It follows that \mathcal{T} must be a unitary operator, i.e., $\mathcal{T}^\dagger = \mathcal{T}^{-1}$.

Our main assumption is that the unperturbed Hamiltonian H_0 from (3) is *translationally invariant* in the sense that the couplings J_{ij} do not depend separately on i and j , but only on the difference $i - j$ (modulo κ). It follows that H_0 is also translationally invariant in the alternative sense that

$$\mathcal{T}^\dagger H_0 \mathcal{T} = H_0, \quad (\text{C1})$$

or, equivalently, $[H_0, \mathcal{T}] = 0$ (commutator). Likewise, one sees that each component of the total spin S^a from (1) is translationally invariant. It follows that all four operators H_0 , S^z , \vec{S}^2 , and \mathcal{T} commute with each other.

Without loss of generality, we thus can assume that the eigenvectors $|n, l\rangle$ of H_0 are at the same time not only eigenvectors of S_z , and \vec{S}^2 , see (4)-(6), but also eigenvectors of \mathcal{T} . Since \mathcal{T} is unitary, the corresponding eigenvalues must be of unit modulus, i.e.,

$$\mathcal{T}|n, l\rangle = e^{i\theta_{n,l}}|n, l\rangle \quad (\text{C2})$$

with certain “phases” $\theta_{n,l} \in [0, 2\pi)$.

Since S^x and S^y commute with \mathcal{T} (see above), the same applies to the raising operator S^+ from (35). Together with (36) it follows that

$$\begin{aligned} S^+ \mathcal{T}|n, l\rangle &= e^{i\theta_{n,l}} S^+|n, l\rangle = e^{i\theta_{n,l}} c_{n,l}^+ |n, l+1\rangle = \\ \mathcal{T} S^+|n, l\rangle &= c_{n,l}^+ \mathcal{T}|n, l+1\rangle = c_{n,l}^+ e^{i\theta_{n,l+1}} |n, l+1\rangle. \end{aligned} \quad (\text{C3})$$

We thus can conclude that $\theta_{n,l+1} = \theta_{n,l}$, and finally that $\theta_{n,l}$ only depends on n , but not on l .

Combining (C2) with the l -independence of $\theta_{n,l}$ one recovers (33) for arbitrary Hermitian operators B . As in the main text, it is *a priori* understood in (33) that $n \in \{1, \dots, N\}$ and $l, l' \in \{-L_n, \dots, L_n\}$, but with the convention adopted below (A14), one readily can extend the same relation to arbitrary n, l, l' .

We finally mention that the choice of the basis as specified below (C1) may in principle not be unique, but that such ambiguities can be excluded if all energies E_n^0 are pairwise different, as it is assumed at the beginning of Sec. IV.

-
- [1] M. Ueda, Quantum equilibration, thermalization and prethermalization in ultracold atoms, *Nat. Rev. Phys.* **2**, 669 (2020).
 - [2] T. Mori, T. N. Ikeda, E. Kaminishi, and M. Ueda, Thermalization and prethermalization in isolated quantum systems: a theoretical overview, *J. Phys. B* **51**, 112001 (2018).
 - [3] C. Gogolin and J. Eisert, Equilibration, thermalization, and the emergence of statistical mechanics in closed quantum systems, *Rep. Prog. Phys.* **79**, 056001 (2016).
 - [4] L. D’Alessio, Y. Kafri, A. Polkovnikov, and M. Rigol, From Quantum Chaos and Eigenstate Thermalization to Statistical Mechanics and Thermodynamics, *Adv. Phys.* **65**, 239 (2016).
 - [5] T. Langen, T. Gasenzer, and J. Schmiedmayer, Prethermalization and universal dynamics in near-integrable quantum systems, *J. Stat. Mech.* 064009 (2016).
 - [6] R. Nandkishore and D. A. Huse, Many-body localization and thermalization in quantum statistical mechanics, *Annu. Rev. Condens. Matter Phys.* **6**, 15 (2015).
 - [7] P. Reimann, Foundation of statistical mechanics under experimentally realistic conditions, *Phys. Rev. Lett.* **101**, 190403 (2008).
 - [8] N. Linden, S. Popescu, A. J. Short, and A. Winter, Quantum mechanical evolution towards equilibrium, *Phys. Rev. E* **79**, 061103 (2009).
 - [9] A. J. Short, Equilibration of quantum systems and subsystems, *New J. Phys.* **13**, 053009 (2011).
 - [10] P. Reimann and M. Kastner, Equilibration of macroscopic quantum systems, *New J. Phys.* **14**, 043020 (2012).
 - [11] A. J. Short and T. C. Farrelly, Quantum equilibration in finite time, *New J. Phys.* **14**, 013063 (2012).
 - [12] B. N. Balz and P. Reimann, Equilibration of isolated many-body quantum systems with respect to general distinguishability measures, *Phys. Rev. E* **93**, 062107 (2016).
 - [13] J. Riddell, N. J. Pagliaroli, and A. Alhambra, Concentration of quantum equilibration and an estimate of the recurrence time, arXiv:2206.07541
 - [14] T. Kinoshita, T. Wenger, and D. S. Weiss, A quantum Newton’s cradle, *Nature* **440**, 900 (2006).
 - [15] H. Bernien et al., Probing many-body dynamics on a 51-atom quantum simulator, *Nature* **551**, 579 (2017).
 - [16] M. C. Banuls, J. I. Cirac, and M. B. Hastings, Strong and weak thermalization of infinite nonintegrable quantum systems, *Phys. Rev. Lett.* **106**, 050405 (2011).
 - [17] C. Li et al., Relaxation of bosons in one dimension and the onset of dimensional crossover, *SciPost Phys.* **9**, 058 (2020).
 - [18] S. Moudgalya, B. A. Bernevig, and N. Regnault, Quantum Many-Body Scars and Hilbert Space Fragmentation: A Review of Exact Results, arXiv:2109.00548; M. Ser-

- byn, D. A. Abanin, and Z. Papić, Quantum many-body scars and weak breaking of ergodicity, *Nat. Phys.* **17**, 675 (2021).
- [19] H. Kim, M. C. Banuls, J. I. Cirac, M. B. Hastings, and D. A. Huse, Slowest local operators in quantum spin chains, *Phys. Rev. E* **92**, 012128 (2015).
- [20] C.-J. Lin and O. I. Motrunich, Quasiparticle explanation of weak-thermalization regime under quench in a nonintegrable quantum spin chain, *Phys. Rev. A* **95**, 023621 (2017).
- [21] T. Farrelly, F. G. S. L. Brandão, and M. Cramer, Thermalization and return to equilibrium on finite quantum lattice systems, *Phys. Rev. Lett.* **118**, 140601 (2017).
- [22] M.P. Zaletel, M. Lukin, C. Monroe, C. Nayak, F. Wilczek, and N.Y. Yao, Colloquium: Quantum and classical discrete time crystals, *Rev. Mod. Phys.* **95**, 031001 (2023)
- [23] P. Hannaford and K. Sacha, A decade of time crystals: quo vadis?, *EPL* **139**, 10001 (2022).
- [24] V. Khemani, R. Moessner, and S. L. Sondhi, A brief history of time crystals, arXiv:1910.10745.
- [25] M. Medenjak, B. Buča, and D. Jaksch, Isolated Heisenberg magnet as a quantum time crystal, *Phys. Rev. B* **102**, 041117(R) (2020).
- [26] H. Watanabe and M. Oshikawa, Absence of quantum time crystals, *Phys. Rev. Lett.* **114**, 251603 (2015).
- [27] H. Watanabe, M. Oshikawa, and T. Koma, Proof of absence of long-range temporal orders in Gibbs states, *J. Stat. Phys.* **178**, 926 (2020).
- [28] Y. Huang, Absence of temporal order in states with spatial correlation decay, arXiv:1912.01210.
- [29] P. Vorndamme, H.-J. Schmidt, C. Schröder, and J. Schnack, Observation of phase synchronization and alignment during free induction decay of quantum spins with Heisenberg interactions, *New J. Phys.* **23**, 083038 (2021).
- [30] A. M. Alhambra, J. Riddell, and L. P. Garcia-Pintos, Time evolution of correlation functions in quantum many-body systems, *Phys. Rev. Lett.* **124**, 110605 (2020).
- [31] K. Bärwinkel, H.-J. Schmidt, and J. Schnack, Structure and relevant dimension of the Heisenberg model and applications to spin rings, *J. Magn. Magn. Mater.* **212**, 240 (2000).
- [32] E. A. Yuzbashyan, B. L. Altshuler, and B. S. Shastri, The origin of degeneracies and crossings in the 1d Hubbard model, *J. Phys. A: Math. Gen.*, **35**, 7525 (2002).
- [33] H. Tasaki, On the local equivalence between the canonical and the microcanonical ensembles for quantum spin systems, *J. Stat. Phys.* **172**, 905 (2018).
- [34] H. Tasaki, From quantum dynamics to the canonical distribution: general picture and rigorous example, *Phys. Rev. Lett.* **80**, 1373 (1998).
- [35] M. Srednicki, The approach to thermal equilibrium in quantized chaotic systems, *J. Phys. A: Math. Gen* **32**, 1163 (1999).
- [36] M. P. Müller, E. Adlam, L. Masanes, and N. Wiebe, Thermalization and canonical typicality in translation-invariant quantum lattice systems, *Commun. Math. Phys.* **340**, 499 (2015).
- [37] J. Z. Imbrie, On Many-Body Localization for Quantum Spin Chains, *J. Stat. Phys.* **163**, 998 (2016).
- [38] R. Gallego, H. Wilming, J. Eisert, and C. Gogolin, What it takes to avoid equilibration, *Phys. Rev. E* **98**, 022135 (2018).
- [39] H. Wilming, M. Goihl, I. Roth, and J. Eisert, Entanglement-ergodic quantum systems equilibrate exponentially well, *Phys. Rev. Lett.* **123**, 200604 (2019).
- [40] C. Booker, B. Buča, and D. Jaksch, Non-stationarity and dissipative time crystals: spectral properties and finite-size effects, *New J. Phys.* **22**, 085007 (2020).
- [41] P. Reimann and J. Gemmer, Why are macroscopic experiments reproducible? Imitating the behavior of an ensemble by single pure states, *Phys. A (Amsterdam)* **552**, 121840 (2020).
- [42] H. De Raedt and K. Michielsen, Computational methods for simulating quantum computers, arXiv:quant-ph/0406210.
- [43] B. Buča, C. Booker, and D. Jaksch, Algebraic theory of quantum synchronization and limit cycles under dissipation, *SciPost Phys.* **12**, 097 (2022).
- [44] E. H. Wichmann and J. H. Crichton, Cluster decomposition properties of the S matrix, *Phys. Rev.* **132**, 2788 (1963).
- [45] S. Weinberg, What is quantum field theory, and what did we think it is?, arXiv:hep-th/9702027
- [46] F. H. L. Essler and M. Fagotti, Quench dynamics and relaxation in isolated integrable quantum spin chains, *J. Stat. Mech.* **6**, 064002 (2016).
- [47] C. Murthy and M. Srednicki, Relaxation to Gaussian and generalized Gibbs states in systems of particles with quadratic Hamiltonians, *Phys. Rev. E* **100**, 012146 (2019).
- [48] M. Gluza, J. Eisert, and T. Farrelly, Equilibration towards generalized Gibbs ensembles for non-interacting systems, *SciPost* **7**, 038 (2019).
- [49] H. Araki, Gibbs states of a one dimensional quantum lattice, *Commun. Math. Phys.* **14**, 120 (1969).
- [50] Y. M. Park, The cluster expansion for classical and quantum lattice systems, *J. Stat. Phys.* **27**, 553 (1982)
- [51] Y. M. Park, and H. J. Yoo, Uniqueness and clustering properties of Gibbs states for classical and quantum unbounded spin systems, *J. Stat. Phys.* **80**, 223 (1995).
- [52] M. Kliesch, C. Gogolin, M. J. Kastoryano, A. Riera, and J. Eisert, Locality of temperature, *Phys. Rev. X* **4**, 031019 (2014).
- [53] J. Fröhlich and D. Ueltschi, Some properties of correlations of quantum lattice systems in thermal equilibrium, *J. Math. Phys. (N.Y.)* **56**, 053302 (2015).